Biointerface Research in Applied Chemistry
Open-Access Journal (ISSN: 2069-5837)

Article
Volume 14, Issue 5, 2024, 119
https://doi.org/10.33263/BRIAC145.119

The Co-Use of Various Forms of Silver and Proteases in the Development of New Dressing Biomaterials for Wound Healing

Anna A. Vaniushenkova [1,*], Daniil Yu. Poberezhniy [1], Natalia S. Panyukova [2], Alexander N. Morozov [3], Sergei V. Kalenov [1], Alexey A. Belov [1]

[1] Department of Biotechnology, Mendeleev University of Chemical Technology of Russia, Moscow, Russia
[2] Department of Isotope Technology and Hydrogen Energy, Mendeleev University of Chemical Technology of Russia, Moscow, Russia
[3] Department of Technology of Inorganic Substances and Electrochemical Processes, Faculty of Technology of Inorganic Substances and High-Temperature Materials, Mendeleev University of Chemical Technology of Russia, Moscow, Russia
* Correspondence: AVaniushenkova@yandex.ru;

Scopus Author ID 57219392083
Received: 21.09.2023; Accepted: 28.01.2024; Published: 21.07.2024

Abstract: A modern complex drug for treating purulent-necrotic wounds should have a sorption capacity, enzymatic, antimicrobial, and antioxidant activities. It is promising to create medicinal antibacterial preparations based on silver nanoparticles with the desired characteristics. They should turn to a great alternative to antibiotics in the wound healing compositions. One of the promising approaches for synthesizing silver nanoparticles is the "green synthesis" by various organisms. The paper discusses the interplay between inorganic and biogenic silver nanoparticles and protease solutions. The effect of various forms of silver on the enzyme activities of proteases in solution has been identified. Biogenic silver nanoparticles have a proven advantage over salt solutions. The mutual influence of enzymes and biocides was studied. The effect of introducing chitosan into the system was also examined. The antioxidant properties of the studied nanoparticles were determined. The biocidal activity of the different silver preparations was demonstrated. The antibacterial activity of biogenic nanoparticles was at or above the activity of chemically synthesized nanoparticles. The results obtained in this work indicate the fundamental possibility of co-immobilization of proteolytic enzyme preparations and silver nanoparticles. Biological activities are maintained throughout the synthesis process.

Keywords: biomaterials; silver nanoparticles; proteases; wound healing.

1. Introduction

A modern complex dressing for the treatment of purulent-necrotic wounds should have a number of properties, e.g., chemisorption of purulent discharge enzymatic, antimicrobial, and antioxidant activity [1,2]. Wound contamination is a common issue when dealing with purulent lesions. The risk of microbial contamination increases with the application, change of bandages, and long-term surgery, coupled with the treatment of patients with disabilities. In view of these, various therapeutic agents (TA) can be used to achieve antibacterial activity.

Silver compounds have been demonstrated to be potent antimicrobial agents with long-term use in medical practice [3,4]. For cutaneous use, nitric acid silver (Ags) solutions are most often used in concentrations of 0.25-5 mass.%.

However, the mechanisms of biocidal action of both ionic forms of silver and its nanoparticles remain not fully understood [5]. It is assumed that silver ions are able to bind thiol groups of various bacterial proteins, preventing them from performing their biological functions. This connection disrupts the paired electron transfer along the respiratory chain. Silver ions probably inhibit DNA replication when interacting with nucleic acids. Significant morphological changes occurring in the microbial cell under the action of ionic silver have been shown. Furthermore, the detachment of the cytoplasmic membrane from the cell wall has been described. The mechanism of antibacterial activity of silver nanoparticles (NPs) differs somewhat from that realized by ionic forms [6]. Presumably, the main target of their action is bacterial membranes. Sorption occurs due to electrostatic interactions [7]. Importantly, the action of nanoparticles leads to a massive loss of intracellular potassium due to a violation of the integrity and general disorganization of the lipid bilayer. Some researchers also associate the effect of nanosilver with certain disorders of the respiratory chain [6,7]. It results in the formation of reactive oxygen species and disruption of the electrochemical gradient due to their production. The dependence of antimicrobial activity of nanoparticles on their shape and size was shown. Moreover, smaller ones have greater cytotoxicity and are found in significant quantities and intracellular compartments. Triangular nanoparticles are known to have a greater damaging effect than spherical ones [6,8].

The necessity to introduce enzymes into the materials for treating various purulent necrotic wounds is sufficiently shown in articles [1,4,9]. Enzymes are known as the most labile components of complex dressings. At the same time, silver nanoparticles are increasingly used as an antimicrobial agent, including in medical practice [3,10-13]. However, heavy metal ions, particularly silver, are strong enzyme inhibitors [14,15].

Ionizable side chain amino acids, especially CO - from peptide bond, COOH, NH, NH_2, N, side chain heteroatoms of serine, threonine, cysteine, and methionine are considered to be capable of binding metal ions. Thus, the number of binding centers will be significant. In addition, the conformation of the protein, as well as the affinity of the metal to the heteroatom and the pH medium's acidity, will determine which donor atoms will bind. Metal may be distributed among several binding centers with different acidity [14].

The metal binding process is considered to be a sequential attachment of metal ions to independent functional macromolecule groups. Possible schemes of metal complex formation of both separate groups (bonds) and macromolecules are given in the literature [16,17]. Moreover, it is known that the pH value influences the binding location of the metal and the biopolymer (protein) [18,19].

A large number of papers have been devoted to the inactivation of enzymes by silver ions [14,15,18-20]. Recently, studies on the effect of various silver NPs on enzymatic activities have aroused interest [6,7,14,19-21]. In addition, many biocides and various TA also affect the activity of enzymes used for medical purposes [1,9].

2. Materials and Methods

2.1. Materials.

Chitosan (Ct), produced by NGOs "Bioprogress" (Shchelkovo, Moscow Region, Russia), was used in the work. The humidity of the polymer is 10%, the degree of deacylation is 80.0%, the kinematic viscosity is not less than 383.7 cSt, and the molecular weight is approximately 500 kDa.

Proteolytic complex from crab' hepatopancreas (PC) manufactured by NGOs "Bioprogress" (Shchelkovo, Moscow Region, Russia). Its casein proteolytic activity is 0.9 PE/mg; BApNa activity is 43 nmol/mg*min; Azocoll activity is 28 units/mg.

Cattle pancreatic trypsin (Tr) produced by "SamsonMed", Russia (FSF 42-0179-5943-04). Its casein proteolytic activity is 7.0 PE/mg; BApNa activity is 3.0 mmol/mg*min).

Bromelain (Brm) is manufactured by the Applied Biotechnology Group of companies (2400 GDU/g). Its casein proteolytic activity is 0.15 PE/mg; BApNa activity is 0.28 nmol/mg*min; Azocoll activity is 7.7 units/mg.

Cattle pancreatic chymopsin (Chm) produced by SamsonMed, Russia. Its casein proteolytic activity is 9.0 PE/mg; BApNa activity is 280 nmol/mg*min; Azocoll activity is 2540 units/mg. Papain (Pap) manufactured by Tayga (Shanghai), China (600TU/mg). Its casein proteolytic activity is 0.4 PE/mg; BApNa activity is 0.1 nmol/mg*min; Azocoll activity is 20 units/mg.

All other reagents, unless specified, are Russian manufactured, with qualifications not lower than high grade.

2.2. Synthesis of nanoparticles.

Manufactured inorganic (NN) NPs (Argentum, PlantoSys, Netherlands) and chemically synthesized silver NPs (InNPs) were used. These InNPs were synthesized by adding sodium borohydride to a solution of silver nitrate and a stabilizer under vigorous stirring. Arabinogalactan as a stabilizer was used.

Biogenic Ag NPs with different compositions and shell thicknesses were obtained by microbiological synthesis. NPs FO and Bulch were synthesized by *Fusarium oxysporum* and *Purpureocillium lilacinum*, respectively [22,23]. Silver nanoparticles (NP-5-2) were synthesized using facultative methylotrophic bacteria Rhodococcus erythropolis. The producer culture was grown in a medium of the following composition (per 1 liter): methanol - 6 ml; yeast extract - 0.1 g; KNO_3 - 1 g; $MgSO_4 \times 7H_2O$ - 0.2 g; $CaCl_2$ - 0.02 g; Na_2HPO_4 - 0.46 g; KH_2PO_4 - 0.35 g; $CuSO_4 \times 5H_2O$ - 0.1 mg; $FeSO_4 \times 7H_2O$ - 2.0 mg; $ZnSO_4 \times 7H_2O$ - 0.1 mg; $Na_2MoO_4 \times 2H_2O$ - 0.03 mg; $CoCl_2 \times 6H_2O$ - 0.2 mg; Na_2EDTA - 5; $MnCl_2 \times 4H_2O$ - 0.03; $NiCl_2 \times 6H_2O$ - 0.02 mg. Cultivation was conducted in Erlenmeyer flasks using an orbital shaker set at 150 rpm and a temperature of 30°C for 1-3 days. At the end of cultivation, the $AgNO_3$ solution was added to the flasks in the amount to achieve a concentration of 50 mg/L Ag^+. The synthesis of nanoparticles was carried out under constant stirring at a temperature of 24–25°C and illumination of 500 lx.

The appearance of the saturated reddish-brown color indicated the completion of the nanoparticles' synthesis. To obtain a pure preparation of nanoparticles, the bacterial cells were separated by centrifugation at 7000 rpm for 10 min, using an Eppendorf 5810R centrifuge. Further, nanoparticles were precipitated from the obtained supernatant by centrifugation. Nanoparticles were resuspended in distilled water and reprecipitated in triplicate to remove all impurities.

2.3. Antibacterial activity.

2.3.1. Bacterial strains.

The activity of silver nanoparticles against *Staphylococcus aureus* and *Bacillus cereus* was tested.

2.3.2. Slot method on the solid medium.

The "slot" method studied the antibacterial activity of the investigated samples. Plating was done on a solid nutrient medium (L-agar) by measuring the growth-inhibiting zone.

Previously, a hollow cylinder 8.0 mm in diameter was placed on the surface of the agar medium. It made creating slots of a given depth and diameter possible. After that, the inoculum used as a test system was added to the surface of the agar nutrient medium in the amount of 0.1 ml. The volume of the applied suspension was spread over the surface of the medium with a sterile spatula. The strain dilution that gives approximately 10^6 CFU/ml per Petri dish, which corresponds to the wound contamination, was used in our study. After seeding, a 100 µl of test solution was placed in the slots. The temperature of the test was 37°C, which equates to the patient's temperature.

The dishes were placed in a thermostat after the samples were placed on the medium seeded with cells. They were incubated for 24 hours at a temperature of 37°C. Then, growth zone delay was measured. During measuring areas, they were guided by full inhibition of visible growth.

2.3.3. Disc diffusion assay.

Nanoparticles were examined for their bactericidal activity using standard microbiology evaluation of the zone of inhibition (ZOI) through the disc diffusion method [24].

2.3.4. Microplate method.

Microbiological studies were carried out using a 96-well plate. The inoculum of the culture was added to the nutrient medium (L-broth) and incubated on a thermostatically controlled shaker Thermo-Shaker PST-60Hl-4, BioSan at 350 rpm, 37°C for 24 hours. 20 µl of culture diluted to the required level, 80 µl of sterile nutrient medium (L-broth), and 100 µl of preparations were added to the plate wells. Every 2 hours, optical density measurements were taken at a wavelength of 505 nm on an iMark microplate photometer from Bio-Rad Lab. Inc., USA, within 24 hours.

2.4. Enzymatic activity.

Enzymatic activities on synthetic substrates BApNa (N-benzoyl-D, L-arginine paranitroanilide), BAEE (N-benzoyl-D, L-arginine ethyl ester), and BocAlaONp (N-butyloxycarbonyl-L-alanyl p-nitrophenyl ester) were determined as described previously [20]. All examinations were performed in 0.2 M acetate buffer solution (0.2 M AcB) pH 6.0-6.2.

Changes in the enzymatic activity (EA) of proteases in the presence of various silver preparations were carried out as follows. Silver preparations and 0.2 M AcB were added to the enzyme solution (in the 0.2 M AcB) to the requested volume. Kept at room temperature for 15 minutes and determined the residual EA.

The number of nanoparticles in the solution was calculated from the optical density of the solution using [22]. The value of the molar extinction coefficient (ε, $l*mol^{-1}*cm^{-1}$) was taken equal to $2*10^4$ at λ_{max}.

2.5. Determination of antiradical activity.

To determine the antiradical activity (AOA) of our preparations, the reaction with a stable free radical 2,2-diphenyl-1-picrylhydrazyl (DPPH) was used [25]. The studies were carried out using a Shimadzu UV-2600 recording spectrophotometer at a wavelength of 517 nm in 1 cm wide cuvettes. A solution of DPPHs (0.2 mmol/l) manufactured by Aldrich was prepared in 96% ethanol. To 2 ml of each of the obtained series solutions, 2 ml of the DPPH solution was poured and mixed after 30 minutes or another specified time; the optical density values were recorded at λ = 517 nm. As control samples, pure solvents were used to prepare working solutions. Working solutions were prepared using sequential dilutions.

We used only freshly prepared solutions. All protein solutions in which turbidity was formed were centrifuged at 20°C for 20 minutes at 14,000 rpm. The formula was calculated as % inhibition:

$$\boldsymbol{Inhibition}\ (\%) = \frac{\boldsymbol{DC_{(0)} - DA_{(t)}}}{\boldsymbol{DC_{(0)}}}\ \boldsymbol{100} \qquad (1)$$

where $DC_{(0)}$ is the optical density of the control sample, and DA(t) is the optical density of the sample.

1 antioxidant activity unit (AOA) is the amount of the drug that causes a 50% inhibition of the DPPH solution under special conditions.

2.6. Instrumentation.

A spectrophotometer (Shimadzu UV-2600), with spectra ranging from 190 to 900 nm and AcB (pH 6.2) as the blank, was used for studying the optical properties.

The FT-IR spectra were obtained with a Nicolet 380 IR Fourier spectrometer (Thermo Scientific, USA) by the ATR method in the 550 – 4000 cm range. The center of the collective usage of the Mendeleev University of Chemical Technology of Russia did measurements.

The surface of the preparations was examined using a JSM JEOL 6510LV microscope. The samples were prepared by depositing a platinum layer 10 nm thick on them using a JFC-1600 magnetron sputtering unit (JEOL, Japan). The deposition was carried out in a vacuum (5 Pa) at a current of 30 mA and a duration of 20 seconds. Argon was used as the purge gas. The samples were taken in secondary electron imaging mode under an accelerating voltage of 15 kV. The Center for the Collective Usage of the Mendeleev University of Chemical Technology of Russia did measurements.

The sizes of nanoparticles were determined on the laser analyzer Nanotrac Ultra 253 (Microtrac, USA) based on a method of dynamic light scattering (DLS).

The TEM was carried out with an electron microscope of JEM-100CX2 (JEOL, Japan). The elemental composition of samples was determined using a JEM-100CX2 electron microscope equipped with an EM-ASID4D scanning unit (JEOL, Japan) and the X-ray microanalyzer (Green Star, Russia) with an E5423 detector (Link-System, UK) under accelerating voltage 80 kV and a tilt angle 35° by energy dispersive X-ray spectroscopy (EDS).

3. Results and Discussion

3.1. Characterization.

UV-visible spectra of the synthesized NPs are demonstrated in Figure 1. They were recorded using 0.2 M acetate buffer in the 190 to 650 nm range. The studied concentrations of

$AgNO_3$, NN, InN, NP-5-2, F.O. and Bulch were $8.5*10^{-4}$M, $6.7*10^{-5}$ M, $5.7*10^{-5}$M, $1.0*10^{-5}$M, $4.6*10^{-5}$M and $1.6*10^{-5}$M, respectively.

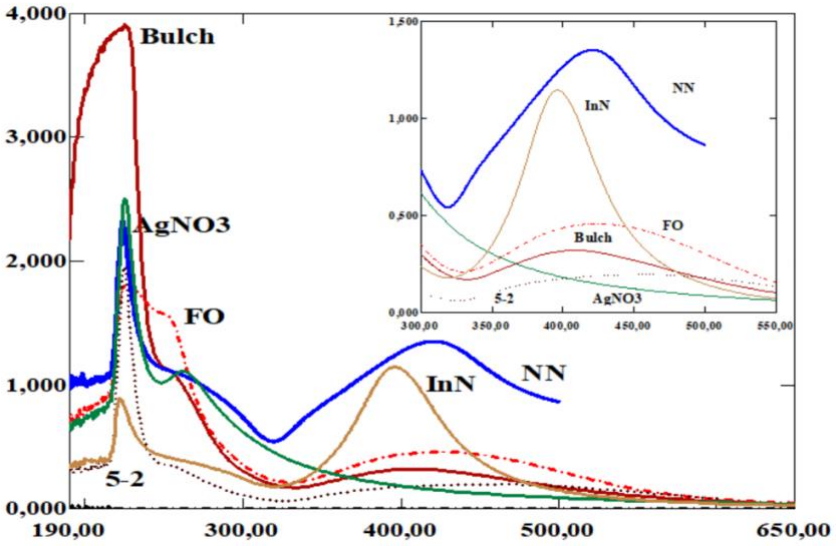

Figure 1. UV-View spectra of silver and various AgNPs described in sub-s 2.2.

The synthesized NPs showed sharp absorption peaks at 390-450 nm (shoulder peak) and 195-220 nm. The obtained silver particles are characterized by intense optical absorption in the region λ=390-450 nm, corresponding to the plasmonic absorption peak of silver [23]. At the same time, the peak observed in the UV region at 300–350 nm is called the B-band and is attributed to the n–π* transition.

The UV–VIS spectra indicated that AgNPs showed a strong absorption of electromagnetic waves in the visible region as a result of the surface plasmon resonance effect. The shift observed in AgNPs could be attributed to the difference in the shape and size distributions of the Ag [23]. Besides, the spectra of the interplay between NPs and enzymes were measured (Figure 2).

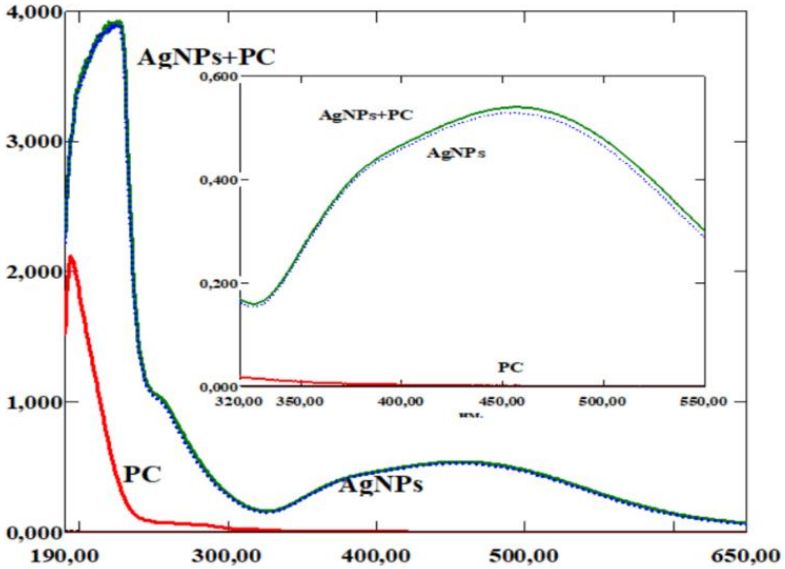

Figure 2. UV-View spectra of interaction between NP-5-2 and PC (the spectra were taken 15 minutes after the injection of the components).

Similar dependences were also obtained for other AgNPs. It should be noted that the interaction time (up to 96 hours) did not significantly affect the spectrum.

FT-IR spectra for all NPs were recorded in the region 500 to 4000 cm^{-1}. The FTIR spectrum of the precursor compound exhibited a vibrational band at 1540–1620 cm^{-1}, which corresponds to C=C stretching and 2870–3020 cm^{-1} to C–H stretching. In addition, a weak band was observed around 3200 cm^{-1}, attributed to a secondary amine [15]. Previously, we discussed the FT-IR spectra for $AgNO_3$ samples and inorganic nanoparticles [15]. The data obtained for biogenic NPs are presented in Figure 3.

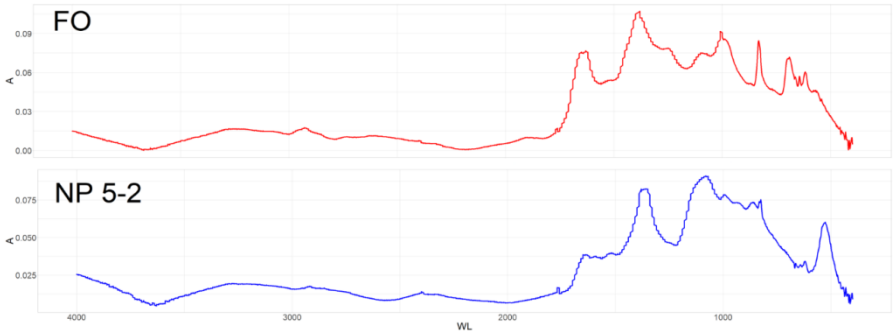

Figure 3. FT-IR spectra of FO and NP-5-2, respectively.

FT-IR spectra for all NPs were recorded in the region 500 to 4000 cm^{-1} (Figure 3). The bands around 3270, 2920, 1760, 1650, 1385, and 1080 cm^{-1} were the peaks of the silver NPs. The FT-IR study of AgNPs showed a peak around 1650 $cm^{-1,}$ demonstrating the presence of amide I. In addition, a weak band was observed around 3100-3200 cm^{-1}, attributed to a secondary amine [15]. Also, peaks around 1385 and 1080 cm^{-1} were observed. They can be related to the C–N stretching vibrations of aromatic and aliphatic amines [26]. Peaks from 3000 to 2850 cm^{-1} were observed because of C-H stretching vibrations of a hydrocarbon skeleton [27].

The size of nanoparticles is one of the main parameters in their creation, in addition to dispersion and chemical stability [28]. The effect of particle size on the antimicrobial effect of silver nanoparticles has been shown in the literature [29]. Smaller nanoparticles (about 15 nm) exhibit higher antibacterial activity against cells of conditionally pathogenic test cultures. The authors [30] suggested that the amounts of chemisorbed silver ions should interpret the mechanism of size-dependent antibacterial activity on the surface of the particles.

Moreover, silver nanoparticles of smaller diameter with a significant ratio of surface area to mass can adsorb more Ag^+ on the surface, which leads to an increase in the antibacterial activity of the particles. In this connection, we conducted experiments to establish the diameters of the studied nanoparticles. The results are shown in Figure 4.

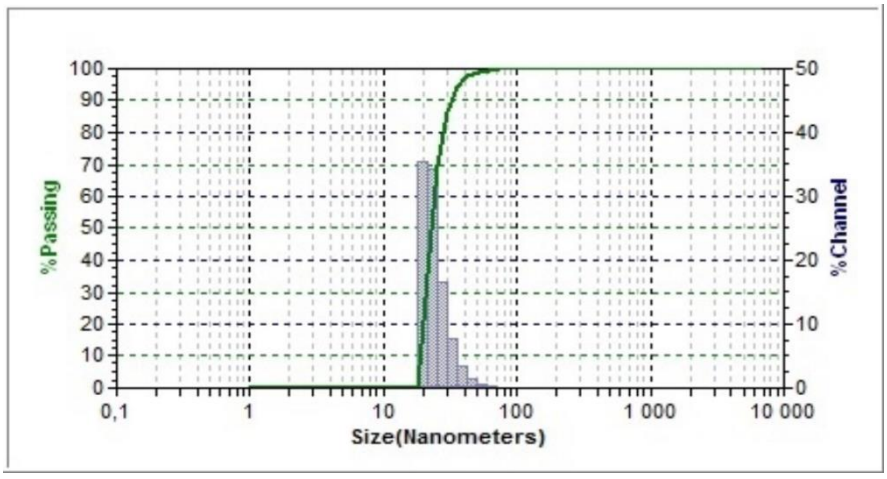

Figure 4. Size distribution histograms of silver NP-5-2 were obtained using the laser diffraction method.

Similar data were obtained for other samples. According to the data, the size of nanoparticles obtained by chemical synthesis (InN) varies from 10 nm to 50 nm (average diameter 19 nm). The Argentum (NN) consists of particles whose sizes range from 20 nm to 150 nm (average diameter 40 nm). The diameters of biogenic FO nanoparticles range from 30 nm to 150 nm (average diameter 56 nm) [31,32]. A low intensity of particle distribution in solution also characterizes these NPs. For NP-5-2, the size of the silver nanoparticles obtained varies in the 16-50 nm ranges, with particles of 16-19 nm in size predominant.

The micrographs of investigated samples were done using transmission electron microscopy (TEM), an effective technique of research of biogenous metal NPs [33]. The data obtained is presented in Figure 5.

The resulting pictures show the NN NPs are square in shape, while the rest of the samples are round.

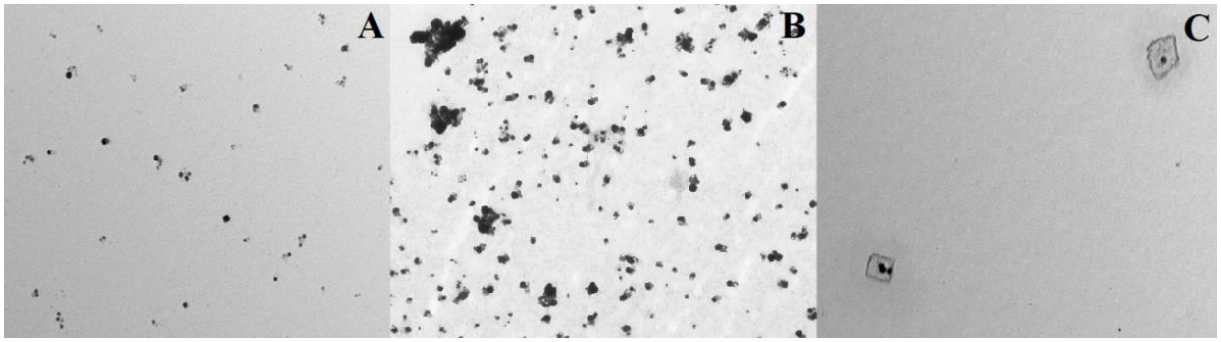

Figure 5. The TEM of NP-5-2, FO, NN, and nanoparticles, respectively.

Also, our previous studies fully characterized silver NPs produced by the fungal cultures isolated from the aerobic activated sludge of wastewater treatment facilities, Fusarium oxysporum [33].

Figure 6 shows SEM micrographs of silver nanoparticles obtained by reaction of the 50 mg/l [Ag^{+}] with the Purpureocillium lilacinum (Bulch) and Rhodococcus erythropolis (NP-5-2) suspensions, respectively after 24 hours.

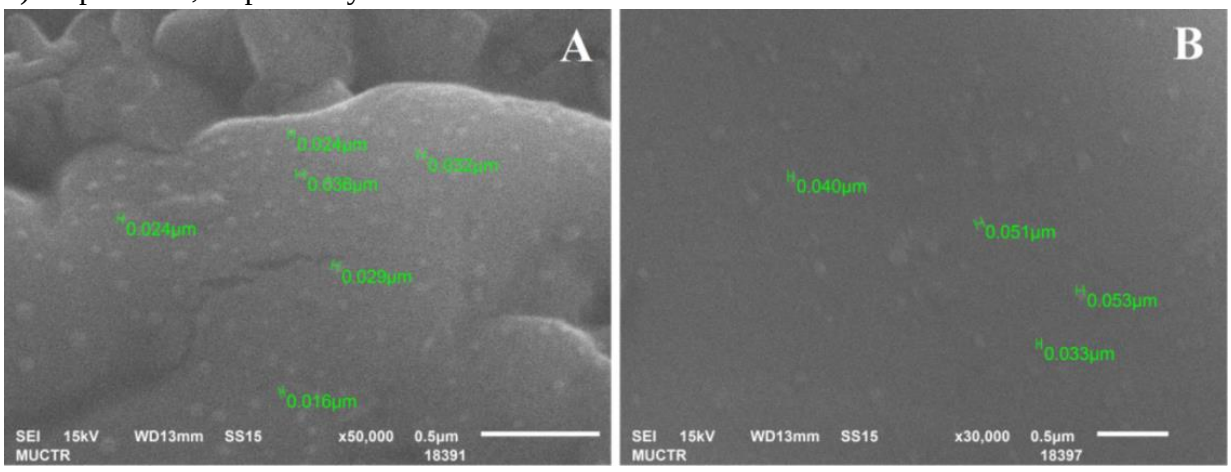

Figure 6. SEM of **(A)** Bulch; **(B)** *NP-5-2* nanoparticles.

As a result, almost spherical, single, or aggregated silver nanoparticles with the following size range were synthesized. Bulch is 16-36 nm, and NP-5-2 is 33-53 nm.

3.2. Silver nitrate solutions' effect ($AgNO_3$) on the enzymes.

Proteases widely spread in medical practice, both in native and immobilized form, were used [1,4]. Besides, the determination of the influence that silver nitrate solution (Ag) exerts

on the studied enzymes was described in detail in sub-s 2.4. The value of enzymatic activity without silver preparations was taken for 100% (1). $AgNO_3$ concentrations cause a 100% substrate activity loss (LD_{100}) were calculated. The data obtained are shown in Table 1. The amount of the enzyme in the sample is indicated in round brackets PC enzymes were subjected to the greatest inactivation due to their ability.

Table 1. LD100 values for various enzymes.

Enzyme	Substrate		
	BApNA	**BAEE**	**BocAlaONp**
PC (0.1 mg)	0.28×10^{-5}M	0.27×10^{-5}M	1.4×10^{-5}M
Tr (0.01 mg)	94×10^{-5}M	-	-
Hmp (0.01 mg)	67×10^{-5}M	14×10^{-5}M	$>100\times10^{-5}$M
Brm (2 mg)	74×10^{-5}M	-	67×10^{-5}M
Pap (1 mg)	1.7×10^{-5}M	-	-

Further studies of the action of AgNPs were carried out on this connection. The data obtained are presented in Table 2.

Table 2. LD_{100} values for PC and various therapeutic agents.

Sample	**Substrate**		
	BApNA	**BAEE**	**BocAlaONp**
PC (0.1 mg)	0.34×10^{-5}M	0.27×10^{-5}M	1.4×10^{-5}M
PC (0.1 mg)-**Ct**	0.7×10^{-5}M	–	–
PC(0.1 mg) + **NN**	0.77×10^{-5}M	–	–
PC(0,1 mg)-**Ct** + **NN**	1.1×10^{-5}M	–	–
PC (0.1 mg)+**InN**	–	–	A/Ao=1 Less than 3.0×10^{-4}M
PC (0.1 mg) +**NP-5-2** (*R. erythropolis*)	0.37×10^{-5}M	–	–
PC (0.1 mg) + **FO**	4.7×10^{-5}M	–	A/Ao=1 Less than 3.6×10^{-6}M
PC (0.1 mg) +**Bulch**	2.5×10^{-5}M	–	–

The molecular weight of the enzymes included in the PC is known to be approximately 23-30 kDa [34-36]. Also, the presence of the hydrocarbon component was not recorded. Collagenases of crustaceans are characterized by an increased content of negatively charged amino acids with a low content of positively charged ones. PC contains various proteinases on top of the true collagenase, as it was established in articles [34,36]. It explains PCs' wide substrate specificity and its' unique therapeutic properties. Silver solutions have a strong inhibitory effect, mostly on PC enzymes. We associate this phenomenon with PCs amino acid content.

Ionizing side chain amino acids, especially CO - from peptide bond, UNS, NH, NH_2, N, side chain heteroatoms of serine, threonine, cysteine, and methionine are considered to be capable of binding metal ions. Thus, the number of binding centers will be significant. In addition, the conformation of the protein, as well as the affinity of the metal to the heteroatom and the pH medium's acidity, will determine which donor atoms will bind. Metal may be distributed among several binding centers with different acidity [19]. The average molecular weight of one amino acid residue is usually taken as 120. The enzymes used have a molecular

weight of 20-30 kDa, i.e., about 200-250 amino acid residues are contained in these enzymes [34-37]. Only available amino acid residues can interact with metal ions. According to articles, cysteine interacts most strongly with silver ions from amino acids [14,20]. The amino group carries out coordination. However, carboxylic sites can also interact with the metal, changing the conformation of enzymes and, subsequently, inactivating them. Table 1 shows a more rapid decrease in enzymatic activity is observed in enzymes with lower isoelectric point values. Since carboxyl groups are predominantly present on the external shell of the enzymes, which are prone to binding heavy metals [19,37,38]. The interaction of FO and InN silver nanoparticles with PC solution was investigated in 0.2 M acetate buffer pH 6.2 as a model of a purulent wound at room temperature for 168 hours. PC solution was used as a control sample in the same concentration and conditions. Consequently, using silver nanoparticles and enzymes together without losing properties is possible.

3.3. Chitosan stabilization of studied enzymes.

Chitosan (Ct) is widely used in modern medicine. For instance, it is used to manufacture medical products containing enzymes [1,4]. Ct has a number of useful properties necessary for wound healing, depending on the molecular weight, degree of deacetylation, source of preparation, etc. [1,39,40]. As was shown in the literature [31,32], the antimicrobial properties of the biogenic nanoparticles are preserved when they are included in various substrates, such as chitosan and sodium alginate. It allows us to hope to create co-immobilized systems like silver NPs and protease without losing biological activity.

The influence of silver preparations on the immobilized Ct gel enzymes was studied (Figure 7). PC was added to the mixture of chitosan and silver nitrate after 15 minutes of exposure to the Ct-Ag composition.

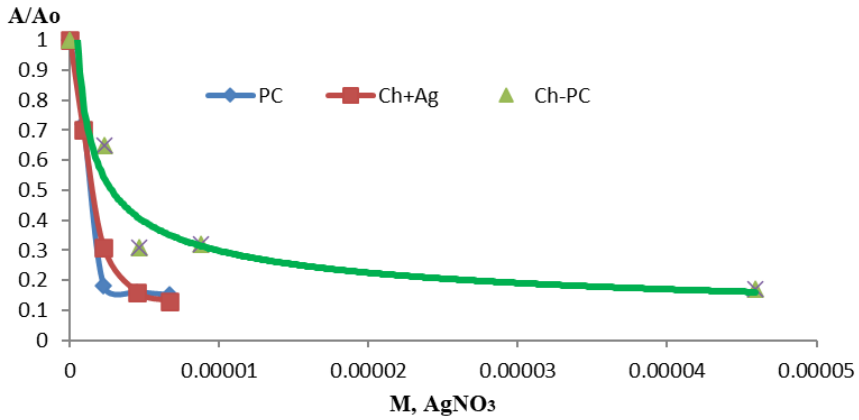

Figure 7. Change in relative enzymatic activity depending on the quantity of silver nitrate supplied.

Ct could form complexes with metal ions due to its chelating properties. When the immobilized enzyme is exposed to the silver preparation solution, Ct chelates Ag ions/atoms and prevents the enzyme from inactivating, as seen in the experiment. When the enzyme is immobilized in the presence of $AgNO_3$, silver cations can be adsorbed on the chitosan macromolecules via the electrostatic (ion-dipole) interactions with oxygen atoms of the hydroxyl and ether groups [41].

The complexation process with NPs can occur due to the participation of chitosan amino groups containing free electron pairs.

As shown in the literature [42], only about 30% of the amino groups of chitosan can react with nucleophiles. This phenomenon means that not all amino groups of Ct are accessible,

even for low molecular weight agents with a multiple excess of the latter. It should also be considered that when Ct interacts with proteases, the polysaccharide can depolymerize, and part of the hidden amino groups can interact with silver ions. This is clearly shown in Figure 7 above.

3.4. Antiradical activity.

The positive effect of antioxidants on preventing infection and healing of purulent wounds, burns, and trophic ulcers is known [43,44].

The process of wound healing, especially the stage of inflammation, occurs under conditions of activation of free radical reactions [1]. Hyperproduction of free radicals in the wound and a decrease in the activity of endogenous antioxidants shift the existing equilibrium toward the acceleration of free radical reactions. In this case, the phenomenon described above is a pathogenetic justification for the exogenous inhibitors' use of free radical reactions as drugs that promote faster wound healing. Definite reports of antioxidant therapy for wounds are presented [45]. Furthermore, the presence of antioxidant activity of metal NPs' formed by amino acids or synthesized with microorganisms was shown in articles [17,46, 47]. The authors associate the presence of free radical quenching activity both with certain amino acids and with the coat that surrounds the metal. We have studied the antioxidative activity of the NPs used. The data obtained are presented in Table 3. Attention should be paid to the pH value when determining antioxidant activity. The pH value should be identical throughout the measurement of a single sample. Therefore, most of the studied samples were made in 1/15 M FB at pH 8.0.

Table 3. Antioxidative activity of studied samples.

Sample	Measured concentrations range	Antioxidative activity
Dihydroquercetin	(1.6-280×10^{-8}M	0.02 mg
Cysteine	0.006-0,29	0.02 mg
Lysine	(0.018-3.6) ×10^{-6}M	∞
Tryptophan	(0.018-3.6) ×10^{-6}M	∞
PC	0.045-1,81	3.4 mg
Tr	0.25-0.98	∞
$AgNO_3$ (sol)	(9.0-922) ×10^{-6}M	∞
NP NN	(2.8-23) ×10^{-6}M	5.1×10^{-5}M
NP InN	(6.3-25) ×10^{-6}M	9.8×10^{-5}M
NP FO	(6.3-23) ×10^{-6}M	2.5×10^{-5}M
NP-5-2	(2.5-100) ×10^{-6}M	2.5×10^{-5}M
NP Bulch	(4-16) ×10^{-6}M	8.6×10^{-5}M

All studied nanoparticles possess a large free radical quenching activity value, as can be seen from the data.

3.5. Antibacterial activity.

The antibacterial activity of silver nanoparticles has been investigated against Gram-positive bacteria, such as *Staphylococcus aureus* and *Bacillus cereus*. To date, the mechanism of action of silver nanoparticles has been investigated, and the reaction process involves the generation of reactive oxygen species (ROS) [48]. Firstly, the developed surface of nanoparticles allows for the generation of large amounts of ROS, increasing the rate of inhibition of the respiratory chain of cells [46,49]. Secondly, the small size contributes to the infusion of NPs into the bacterial cell, causing damage to the membranes. In addition, the NPs coat allows for the prolongation of the process of silver ion release.

Initially, an evaluation experiment was carried out using the slot method. Figure 8 shows data obtained for sample NP-5-2.

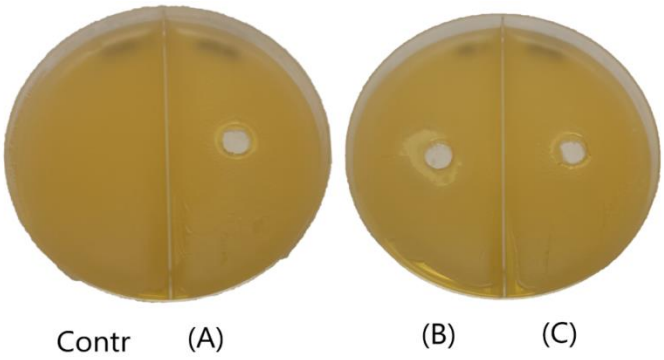

Figure 8. Antibacterial activity of **(A)** NP-5-2; **(B)** NP-5-2 with the addition of Ct; **(C)** NP-5-2 with the addition of PC.

The data show that introducing the enzyme into the system does not significantly affect the NP's activity. The introduction of Ct, on the contrary, contributes to an increase in bactericidal action. This phenomenon is also widely observed [50,51].

Green silver nanoparticles synthesized using Rhodococcus erythropolis and Fusarium oxysporum as producers had different effects on the diameter of the growth inhibition zone of test cultures. An increase in the concentration of synthesized silver nanoparticles also increased the diameter of the inhibition zone (Figure 9).

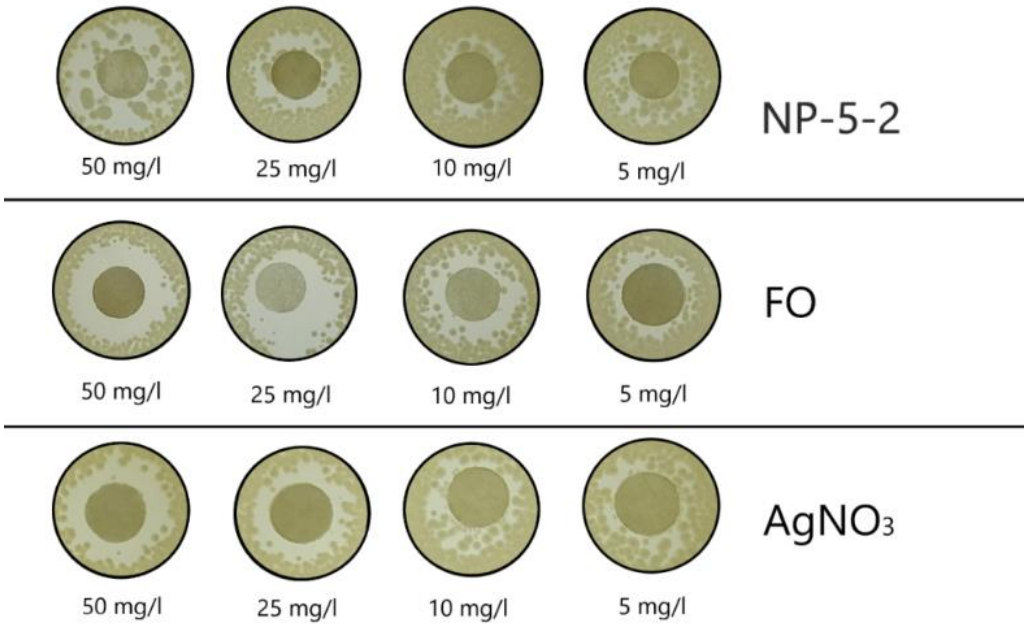

Figure 9. Antibacterial activity of NP-5-2, FO, $AgNO_3$.

Figure 9 shows that low concentrations did not show any significant activity against *S. aureus*, so 25-50 mg/ml diapason was considered the most interesting for future investigations. An experiment was conducted using a microplate photometer to detail the inhibiting process of the conditionally pathogenic test cultures. The studied concentrations of $AgNO_3$, NN, NP-5-2, F.O. and Bulch were $1.6*10^{-7}$M, $1.5*10^{-4}$M, $2.9*10^{-5}$M, $2.2*10^{-5}$ M and $3.5*10^{-5}$M, respectively. The data obtained are presented in Figure 10.

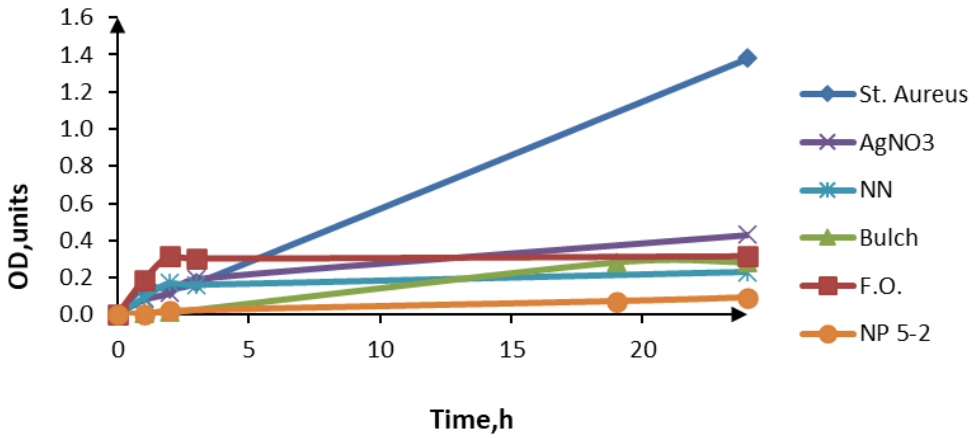

Figure 10. Growth and inhibition curves of *S. aureus* at 4×10^6 CFU/ml concentration with studied silver nanoparticles.

The data presented above showed a greater antibacterial activity of NP-5-2 against Staphylococcus aureus compared to other samples, which increases with increased concentration and number of nanoparticles. However, all biogenic nanoparticles showed a greater or equal inhibitory effect than those obtained by chemical synthesis.

Similar data were obtained against *B. cereus.*

4. Conclusions

It was found that the silver nanoparticles do not have an inactivating effect on the studied enzymes, unlike the silver solution. Consequently, it is possible to use silver nanoparticles and enzymes together without losing properties. Furthermore, resulting solutions have antimicrobial properties.

Funding

This research received no external funding.

Acknowledgments

The authors acknowledge the Mendeleev University of Chemical Technology of Russia for providing means and resources. We are grateful for assistance from Centre of the collective usage of the Mendeleev University of Chemical Technology of Russia.

Conflicts of Interest

The authors declare no conflict of interest.

References

1. Belov, A.A. Textile materials containing immobilized hydrolases for medical and cosmetic purposes. Receipt. Properties. Application; LAP LAMBERT Acad. Pub., GmbH &Co. KG, Germany, **2012**.
2. Nguyen, H.M.; Le, T.T.N.; Nguyen, A.T.; Le, H.N.T.; Pham, T.T. Biomedical materials for wound dressing: recent advances and applications. *RSC Adv.* **2023**, *13*, 5509-5528, https://doi.org/10.1039/D2RA07673J.
3. Shcherbakov, A.B.; Kortschak, H.Y.; Surmasheva, E.W.; Skorokhod, Y.M. Silver preparations: Yesterday, today, tomorrow. *Pharm. J.* **2006**, *5*, 45–57.
4. State pharmacopeia of the Russian Federation. Mashkovsky M. D. Moscow: Novaya Volna, **2012**.

5. Zharkova, M.S. Combined action of proteins and peptides of the innate immune system and compounds of various chemical nature in the implementation of their antibiotic properties. PhD Diss., Institute of Experimental Medicine, S-Peterburg, RU, **2016**.
6. Durán, N.; Marcato, P.D.; De Conti, R.; Alves, O.L.; Costa, F.T.M.; Brocchi, M. Potential use of silver nanoparticles on pathogenic bacteria, their toxicity and possible mechanisms of action. *J. Braz. Chem. Soc.* **2010**, *21*, 949–959, https://doi.org/10.1590/s0103-50532010000600002.
7. Lara, H.H.; Garza-Treviño, E.N.; Ixtepan-Turrent L.; Singh, D.K. Silver nanoparticles are broad-spectrum bactericidal and virucidal compounds. *J. Nanobiotechnology* **2011**, *9*, 30, https://doi.org/10.1186/1477-3155-9-30.
8. Kurek, A.; Grudniak, A.M.; Kraczkiewicz-Dowjat, A.; Wolska, K.I. New Antibacterial Therapeutics and Strategies. *Pol. J. Microbiol.* **2011**, *60*, 3–12, http://doi.org/10.33073/pjm-2011-001.
9. Vaniushenkova, A.A.; Khabibulina, N.V.; Morozov, A.N.; Belov, A.A. Synthesis and study of the properties of composite materials based on cellulose and chitosan containing various therapeutic agents. Part 4. Study of the processes of destruction of dressings based on modified cellulose in conditions simulating a purulent-necrotic wound. *Butlerov Communications C* **2021**, *1*, https://doi.org/10.37952/ROI-jbc-C/21-1-2-8.
10. Parmar, S.; Kaur, H.; Singh, J.; Matharu, A.S.; Ramakrishna, S.; Bechelany, M. Recent Advances in Green Synthesis of Ag NPs for Extenuating Antimicrobial Resistance. *Nanomaterials* **2022**, *12*, 1115, https://doi.org/10.3390/nano12071115.
11. Ye, L.; Cao, Z.; Liu, X.; Cui, Z.; Li, Z.; Liang, Y.; Zhu, S.; Wu, S. Noble metal-based nanomaterials as antibacterial agents. *J. Alloys Compd.* **2022**, *904*, 164091, https://doi.org/10.1016/j.jallcom.2022.164091.
12. Murillo-Rábago, E.I.; Vilchis-Nestor, A.R.; Juarez-Moreno, K.; Garcia-Marin, L.E.; Quester, K.; Castro-Longoria, E. Optimized Synthesis of Small and Stable Silver Nanoparticles Using Intracellular and Extracellular Components of Fungi: An Alternative for Bacterial Inhibition. *Antibiotics* **2022**, *11*, 800, https://doi.org/10.3390/antibiotics11060800.
13. Nicolae-Maranciuc, A.; Chicea, D.; Chicea, L.M. Ag Nanoparticles for Biomedical Applications—Synthesis and Characterization.—A Review. *Int. J. Mol. Sci.* **2022**, *23*, 5778, https://doi.org/10.3390/ijms23105778.
14. Russell, A.D.; Hugo, W.B. 7 Antimicrobial Activity and Action of Silver. *Prog. Med. Chem.* **1994**, *31*, 351-370, https://doi.org/10.1016/S0079-6468(08)70024-9.
15. Vaniushenkova, A.A.; Shokodko, M.I.; Kushnerev, K.S.; Panyukova, N.S.; Kalenov, S.V.; Poberezhniy, D.Y.; Belov, A.A. THE SILVER NANOPARTICLES AND PROTEASES IN THE USE OF CREATIONOF NEW WOUND HEALING BIOMEDICAL MATERIALS. *Chemical Industry Today* **2023**, 14-23, http://doi.org/10.53884/27132854_2023_1_14.
16. Sigel, H.; Gemant, A. Metal Ions in Biological Systems, Volume 8: Nucleotides and Derivatives: Their Ligating Ambivalency. *Journal of The Electrochemical Society*. **1980,** *127*, 5, https://doi.org/10.1149/1.2129855.
17. Nga, N.T.T.; Tran, H.V.; Dang, C.H. An Investigation on the Synthesis, Structure and Specific Properties of Zn(II) and Cu(II) Complexes with Tryptophan. *Biointerface Res. Appl. Chem.* **2023**, *13*, 2, http://doi.org/10.33263/BRIAC131.002.
18. Bezrukov, M.G.; Belousova, A.M.; Sergeev, V.A. The Interaction of Metals with Proteins. *Russ. Chem. Rev.* **1982**, *51*, 397, https://doi.org/10.1070/RC1982v051n04ABEH002849.
19. Lopatin, S.A.; Varlamov, V.P.; Davankov, V.A. Ligand exchange chromatography of proteins and enzymes. *Bioorg. Khim.* **1990**, *16*, 725–750.
20. Liau, Y.A.; Read, D.C.; Pugh, W.J.; Furr, J.R.; Russell, A.D. Interaction of silver nitrate with readily identifiable groups: relationship to the antibacterial action of silver ions. *Lett. Appl. Microbiol.* **1997**, *25*, 279–283, https://doi.org/10.1046/j.1472-765X.1997.00219.x.
21. Chambers, J.L.; Christoph, G.G.; Krieger, M.; Kay, L.; Stroud, R.M. Silver ion inhibition of serine proteases: Crystallographic study of silver--trypsin. *Biochem. Biophys. Res. Commun.* **1974**, *59*, 70-74, https://doi.org/10.1016/S0006-291X(74)80175-0.
22. Glavind, J. Antioxidants in Animal Tissue. *Acta Chem. Scand.* **1963**, *17*, 1635-1640, https://doi.org/10.3891/acta.chem.scand.17-1635.
23. Abdellatif, A.A.H.; Alturki, H.N.H.; Tawfeek, H.M. Different cellulosic polymers for synthesizing silver nanoparticles with antioxidant and antibacterial activities. *Sci. Rep.* **2021**, *11*, 84, https://doi.org/10.1038/s41598-020-79834-6.

24. Drew, W.L.; Barry, A.L.; O'Toole, R.; Sherris, J.C. Reliability of the Kirby-Bauer Disc Diffusion Method for Detecting Methicillin-Resistant Strains of *Staphylococcus aureus*. *Appl. Microbiol.* **1972**, *24*, 240-247, https://doi.org/10.1128/am.24.2.240-247.1972.
25. Ershov, B.G. Metal nanoparticles in aqueous solutions: electronic, optical and catalytic properties. Ros. him. zh., **2001**, 45(3), 20-30
26. Otari, S.V.; Patil, R.M.; Ghosh, S.J.; Thorat, N.D.; Pawar, S.H. Intracellular synthesis of silver nanoparticle by actinobacteria and its antimicrobial activity. *Spectrochim. Acta - A: Mol. Biomol. Spectrosc.* **2015**, *136*, 1175-1180, https://doi.org/10.1016/j.saa.2014.10.003.
27. Zayed, M.F.; Mahfoze, R.A.; El-Kousy, S.M.; Al-Ashkar, E.A. *In-vitro* antioxidant and antimicrobial activities of metal nanoparticles biosynthesized using optimized *Pimpinella anisum* extract. *Colloids Surf. A: Physicochem. Eng. Asp.* **2020**, *585*, 124167, https://doi.org/10.1016/j.colsurfa.2019.124167.
28. Hadji, H.; Bouchemal, K. Effect of micro-and nanoparticle shape on biological processes. *J. Control. Release* **2022**, *342*, 93-110, https://doi.org/10.1016/j.jconrel.2021.12.032.
29. Baker, C.; Pradhan, A.; Pakstis, L.; Pochan, D.J.; Shah, S.I. Synthesis and Antibacterial Properties of Silver Nanoparticles. *J. Nanosci. Nanotechnol.* **2005**, *5*, 244-249, https://doi.org/10.1166/jnn.2005.034.
30. Lok, C.-N.; Ho, C.-M.; Chen, R.; He, Q.-Y.; Yu, W.-Y.; Sun, H.; Tam, P.K.-H.; Chiu J.-F.; Che, C.-M. Silver nanoparticles: partial oxidation and antibacterial activities. *JBIC J. Biol. Inorg. Chem.* **2007**, *12*, 527–534, https://doi.org/10.1007/s00775-007-0208-z.
31. Gordienko, M.G.; Palchikova, V.V.; Kalenov, S.V.; Lebedev, E.A.; Belov, A.A.; Menshutina, N.V. The alginate–chitosan composite sponges with biogenic Ag nanoparticles produced by combining of cryostructuration, ionotropic gelation and ion replacement methods. *Int. J. Polym. Mater. Polym. Biomater.* **2022**, *71*, 34-44, https://doi.org/10.1080/00914037.2020.1798439.
32. Gordienko, M.G.; Palchikova, V.V.; Kalenov, S.V.; Belov, A.A.; Lyasnikova, V.N.; Poberezhniy, D.Y.; Chibisova, A.V.; Sorokin, V.V.; Skladnev, D.A. Antimicrobial activity of silver salt and silver nanoparticles in different forms against microorganisms of different taxonomic groups. *J. Hazard. Mater.* **2019**, *378*, 120754, https://doi.org/10.1016/j.jhazmat.2019.120754.
33. Tyupa, D.V.; Kalenov, S.V.; Baurina, M.M.; Yakubovich, L.M.; Morozov, A.N.; Zakalyukin, R.M.; Sorokin, V.V.; Skladnev, D.A. Efficient continuous biosynthesis of silver nanoparticles by activated sludge micromycetes with enhanced tolerance to metal ion toxicity. *Enzyme Microb. Technol.* **2016**, *95*, 137-145, https://doi.org/10.1016/j.enzmictec.2016.10.008.
34. Litvin, F.E. Collagenolytic proteases from the hepatopancreas of the king crab; selection and properties. PhD Diss., Moscow State Forest University, M., RU, **1993**.
35. Klimova, O.A.; Vedischeva, I.V.; la Strongin, A. Isolation and characterization of collagenolytic enzymes from the hepatopancreas of snow crab Chionoecetes Opilio. *Dokl. Akad. Nauk. SSSR.* **1991**, *317*, 482-484.
36. Rudenskaya, G.N.; Isaev, V.A.; Shmoylov, A.M.; Karabasova, M.A.; Shvets, S.V.; Miroshniko, A.I.; Brusov, A.B. Preparation of proteolytic enzymes from kamchatka crab *Paralithodes camchatica* hepatopancreas and their application. *Appl. Biochem. Biotechnol.* **2000**, *88*, 175–183, https://doi.org/10.1385/ABAB:88:1-3:175.
37. Mosolov, V.V. Proteolytic enzymes, M.: Nauka, RU, **1971**, 404.
38. Gimaeva, A.R.; Valinurova, E.R.; Igdavletova, D.K.; Kudasheva, F.Kh.; Sorption of heavy metal ions from water by activated carbon adsorbents. Sorption and chromatographic processes, **2011**, 11, 350-356.
39. Liu, Z.; Xu, Y.; Su, H.; Jing, X.; Wang, D.; Li, S.; Chen, Y.; Guan, H.; Meng, L. Chitosan-based hemostatic sponges as new generation hemostatic materials for uncontrolled bleeding emergency: Modification, composition, and applications. *Carbohydr. Polym.* **2023**, *311*, 120780, https://doi.org/10.1016/j.carbpol.2023.120780.
40. Ressler, A. Chitosan-Based Biomaterials for Bone Tissue Engineering Applications: A Short Review. *Polymers* **2022**, *14*, 3430, https://doi.org/10.3390/polym14163430.
41. Saifuddin, N.; Nian, C.Y.; Zhan, L.W.; Ning, K.X. Chitosan-silver Nanoparticles Composite as Point-of-use Drinking Water Filtration System for Household to Remove Pesticides in Water. *Asian J. Biochem.* **2011**, *6*, 142-159, https://doi.org/10.3923/ajb.2011.142.159.
42. Rinaudo, M. Chitin and chitosan: Properties and applications. *Prog. Polym. Sci.* **2006**, *31*, 603-632, https://doi.org/10.1016/j.progpolymsci.2006.06.001.
43. Grisham, M.B. Oxidants and free radicals in inflammatory bowel disease. *Lancet* **1994**, *344*, 859-861, https://doi.org/10.1016/s0140-6736(94)92831-2.
44. Halliwell, B. Free radicals, antioxidants, and human disease: curiosity, cause, or consequence? *Lancet* **1994**, *344*, 721-724, https://doi.org/10.1016/S0140-6736(94)92211-X.

45. Kamaev, M. F. An infected wound and its treatment. Moscow : Medgiz, **1962**.
46. Faisal, S.; Sadiq, S.; Mustafa, M.; Khan, M.H.; Sadiq, M.; Iqbal, Z.; Khan, M. Tailoring the antibacterial and antioxidant activities of iron nanoparticles with amino benzoic acid. *RSC Sustain.* **2023**, *1*, 139–146, https://doi.org/10.1039/D2SU00044J.
47. Soliman, M.K.Y.; Salem, S.S.; Abu-Elghait, M.; Azab, M.S. Biosynthesis of Silver and Gold Nanoparticles and Their Efficacy Towards Antibacterial, Antibiofilm, Cytotoxicity, and Antioxidant Activities. *Appl. Biochem. Biotechnol.* **2023**, *195*, 1158-1183, https://doi.org/10.1007/s12010-022-04199-7.
48. Skwarczynski, M.; Bashiri, S.; Yuan, Y.; Ziora, Z.M.; Nabil, O.; Masuda, K.; Khongkow, M.; Rimsueb, N.; Cabral, H.; Ruktanonchai, U.; Blaskovich, M.A.T.; Toth, I. Antimicrobial Activity Enhancers: Towards Smart Delivery of Antimicrobial Agents. *Antibiotics* **2022**, *11*, 412**,** https://doi.org/10.3390/antibiotics11030412.
49. Kotarkonda, L.K.; Sinha, T.P.; Bhoi, S.; Tyagi, A.; Kumar, A.; Singh, V.P.; Bharathala, S. Chapter 3 - Nanoparticles as potential antimicrobial agents for enzyme immobilization in antimicrobial wound dressings. In Antimicrobial Dressings; Khan, R., Gowri, S., Eds.; Academic Press, **2023**; 43-60, https://doi.org/10.1016/B978-0-323-95074-9.00009-9.
50. Mohammed, A.M.; Hassan, K.T.; Hassan, O.M. Assessment of antimicrobial activity of chitosan/silver nanoparticles hydrogel and cryogel microspheres. *Int. J. Biol. Macromol.* **2023**, *233*, 123580, https://doi.org/10.1016/j.ijbiomac.2023.123580.
51. Hermosilla, E.; Díaz, M.; Vera, J.; Contreras, M.J.; Leal, K.; Salazar, R.; Barrientos, L.; Tortella, G.; Rubilar, O. Synthesis of Antimicrobial Chitosan-Silver Nanoparticles Mediated by Reusable Chitosan Fungal Beads. *Int. J. Mol. Sci.* **2023**, *24*, 2318, https://doi.org/10.3390%2Fijms24032318.